

# (I-1) Evolution of surface melt damage, its influence on plasma performance and prospects of recovery

J.W. Coenen<sup>a</sup>, K.Krieger<sup>b</sup>, B.Lipschultz<sup>c</sup>, R.Dux<sup>b</sup>, A.Kallenbach<sup>b</sup>, T.Lunt<sup>b</sup>, H.W. Mueller<sup>b</sup>, S.Potzel<sup>b</sup>, R.Neu<sup>b</sup>, A.Terra<sup>a</sup>,  
and the ASDEX Upgrade and TEXTOR Teams

<sup>a</sup>Institute of Energy and Climate Research - Plasma Physics, Forschungszentrum Jülich, EURATOM Association, Trilateral Euregio Cluster, Jülich, GERMANY

<sup>b</sup>Max-Planck-Institut für Plasmaphysik, EURATOM Assoziation, Garching, GERMANY

<sup>c</sup>Massachusetts Institute of Technology, Plasma Science & Fusion Center, Cambridge, USA

---

## Abstract

Experiments have been carried out in the TEXTOR, ASDEX Upgrade (AUG) and Alcator C-Mod (C-Mod) tokamaks to study melt-layer motion, macroscopic W-erosion from the melt as well as the changes of material properties such as grain-size and voids. In addition the effect of multiple exposures is studied to judge the potential amelioration of inflicted melt damage. The parallel heat flux at the radial position of the PFCs in the plasma ranges from around  $q_{\parallel} \sim 45 \text{ MW/m}^2$  at TEXTOR up to  $q_{\parallel} \sim 500 \text{ MW/m}^2$  at C-Mod which covers scenarios close to ITER parameters, allowing samples to be exposed and molten even at shallow divertor angles. Melt-layer motion perpendicular to the magnetic field is observed consistent with a Lorentz-force originating from thermoelectric emission of the hot sample. While melting in the limiter geometry at TEXTOR is rather quiescent causing no severe impact on plasma operation, exposure in the divertors of AUG and C-Mod shows significant impact on operation, leading to subsequent disruptions. The power-handling capabilities are severely degraded by forming exposed hill structures and changing the material structure by re-solidifying and re-crystallizing the original material. Melting of W seems highly unfavorable and needs to be avoided especially in light of uncontrolled transients and misaligned PFCs.

## Keywords:

PSI-20: Alcator C-Mod, ASDEX Upgrade, Divertor geometry, Melting

PACS: 52.55.Rk, 52.40.Hf, 52.55.Fa, 52.25.Vy

---

## 1. Introduction

Tungsten (W) will be used as plasma facing armor material for the ITER divertor and is also the most promising option for the first wall of DEMO. However, use of metallic PFCs (e.g. W) imposes constraints on power-handling due to possible melting by uncontrolled thermal loads. The resulting damage may hamper subsequent operation due to reduced thermo-mechanical resilience of the re-solidified surface and can also lead to increased erosion and thus increased radiation cooling of the core plasma by influx of high-Z impurities. Previous experiments with test-limiters in TEXTOR [1, 2, 3] revealed that melting may cause a strong tungsten source as well as surface modifications which increase by being exposed to ever higher heat flux (impact angle change). Cooling of the main plasma followed by a plasma disruptions is, however, not typical except for events with ejection of large droplets ( $> 10 \mu\text{m}$ ). The evolution of melt damage at castellated divertor structures has of yet been studied only in plasma gun experiments. In addition studies have been performed on the motion of ejected droplets, as well as their plasma impact and divertor screening of W material influx in the tokamak AUG by melting W-pins at the outer strike point

[4]. Accidental melting of tungsten divertor components in the C-Mod divertor showed that it is hardly possible to run high performance plasmas on severely damaged W components due to the degradation of plasma performance. To investigate the detrimental effects of melt-layer formation on surface integrity and plasma impurity contamination in more detail, dedicated experiments with controlled, induced melting of castellated W structures were performed in AUG.

Before describing the most recent results from divertor tokamak experiments we present a short overview of the available conclusions and observations from several TEXTOR experiments. During steady state plasmas  $2 \text{ mm}$  thick, thermally isolated W-plates were exposed to the edge plasma at  $36^\circ$  causing roughly  $20 \text{ MW/m}^2$  to impinge [1]. The nature of melt layer motion was identified to be dominated by  $j \times B$  forces caused by thermo-electric emission [5] moving the melt perpendicular to the magnetic field. This caused a strong re-distribution of molten material and re-solidification into hill like structures now even more exposed to the heat flux. With a melt layer of roughly  $1 \text{ mm}$  depth castellations are bridged and strong changes to the material structure occur [6]. Subsequent tests under transient conditions show a strong deterioration in terms of power handling, crack behavior and performance under thermal cycling [2, 6]. No benign smoothing of leading edges or recovery from melt damage is observed [1, 2].

---

Email address: j.w.coenen@fz-juelich.de (J.W. Coenen)

URL: fz-juelich.de/IEF/IEF-4 (J.W. Coenen)

As the TEXTOR experiments have been performed under rather forced conditions, namely a field line angle close to perpendicular to the surface, steady state, thermally isolated samples as well as limiter geometry, further experiments and studies under divertor conditions, ideally ELMy H-Modes are needed. The main differences are the impinging angle of the heat flux and magnetic field, castellation geometry and the impact on plasma operation due to screening of impurities being different in divertor geometry as seen in previous pin-melt exposures at AUG [4, 7]. In this contribution mainly two 'experiments' are considered: firstly, accidental melting during tungsten dedicated run campaigns ('07-'09) in C-Mod as well as the dedicated exposures of castellated structures with an inherent leading edge at AUG.

This paper is structured as follows: The experiments and setups at AUG and C-Mod are described in section 2 followed by the Experimental Results (Sec. 3), in the end Conclusions and a short outlook are presented (Sec. 4).

## 2. Experiments

In this section the experimental conditions in the two devices (C-Mod and AUG) used are described. Here both the melting under controlled conditions as well as accidental melt exposure are considered. While the melt events in C-Mod are caused by accidental exposure of parts of the installed W-PFCs dedicated construction of melt samples for AUG was undertaken. In both cases the melt layer motion, melt layer damage, as well as material structure and melt layer losses have been studied.

### 2.1. Alcator C-Mod

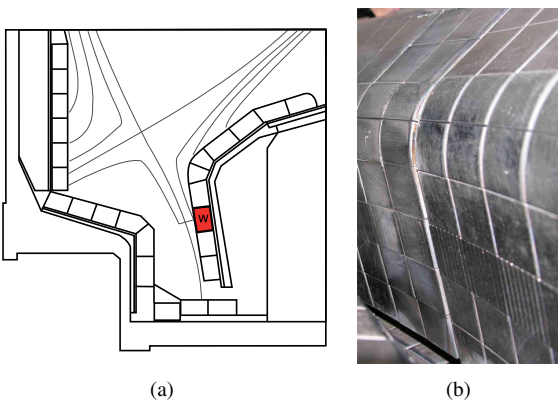


Figure 1: C-Mod outer divertor and tungsten row location

A full toroidal row of tungsten tiles was installed in the outer divertor (Fig. 1) for three run campaigns in order to study the impact of tungsten on plasma operation and W erosion and migration [8]. In contrast to the mono-block design used for the molybdenum PFCs the tungsten row consisted of single lamellae 2(a) sized  $(20 \times 28 \times 4) \text{ mm}^3$ . A set of 8 lamellae makes up one 'tile' block bolted to the divertor substructure 2(b). Extensive thermal simulations have been performed to

establish a stable design usable in the High-Power C-Mod discharges. Typical plasma parameters during those experiments were:  $I_p = 1 \text{ MA}$ ,  $B_T = 5.1 \text{ T}$ ,  $P_{ICRH} = 5 \text{ MW}$  allowing for  $300 - 500 \text{ MW/m}^2$  of parallel heat flux impinging on the target. As the impact angle is lower than  $1^\circ$  the design shown in figure 2(b) is able to withstand the perpendicular heat flux which has much reduced ( $q_\perp \ll q_\parallel$ ) without any problems. During the whole 2007/2008 run campaigns no issues were observed [8, 9]. During the shutdown prior to the 2009 run campaign

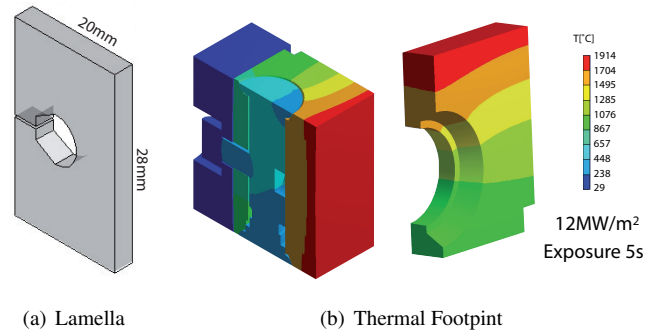


Figure 2: Alcator C-Mod tungsten lamella design

bolting of several W-tile sets was performed inadequately leading to the total loss of one 8-lamella set and subsequent exposure of the neighboring set which was tilted into the SOL plasma stream but didn't fall out (fig. 7(b)). Here the damage of those lamellae is studied wrt. material structure changes as well as forces operating on the melt - only a short outlook on the impact on plasma operation is given as it is described in detail in [9]. Multiple melt occurrences are observed including strong disruptions, finally preventing high-power H-mode operation with the outer strike point on the damaged component.

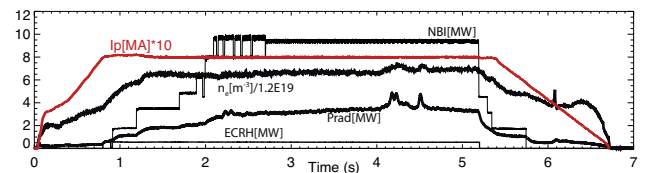


Figure 3: Typical parameter traces during melt exposure at AUG (#27377)

### 2.2. ASDEX Upgrade

In contrast to the accidental melting in C-Mod in AUG intentionally misaligned castellated tungsten structures (1.5mm height) were exposed at the outer target plate using the AUG divertor manipulator in the middle of divertor sector 2. Plasma flux and temperature were measured by flush-mounted Langmuir probes [10] in sector 8 (i.e.  $135^\circ$  toroidally from the pin position). Spectral line emission in the visible range at the sample exposure location was detected by an array of optical fibres (figure 11) viewing the sample surface from below the dome baffle with the attached spectrometer tuned to the wavelength range around the tungsten WI line at 400.9 nm [11]. Three

discharges (#27377-#27379) with the divertor manipulator in place were performed during which the strike point was moved from a position roughly 9cm below the manipulator onto the exposed sample. The melting was induced during an ELMy H-Mode divertor discharge ( $I_P = 0.8MA$ ,  $B_T = 2.5T$ ,  $P_{NBI} = 10MW$ ,  $q_{||} = 80MW/m^2$ ). The divertor manipulator is located

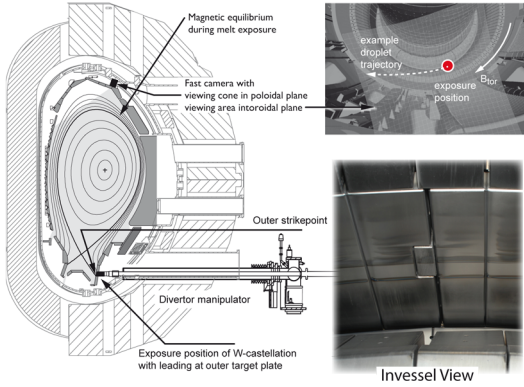


Figure 4: AUG divertor manipulator, setup and geometry

in the outer divertor (Fig. 4) allowing to expose samples or probes to the divertor plasma under the true divertor geometry - the samples are aligned with the surrounding divertor surfaces. Melting will only occur under somewhat forced conditions. With the Manipulator surface flush-mounted the field lines typically impinging under  $3^\circ$  the perpendicular heat flux is in the range of  $4 - 5MW/M^2$  ( $q_{||} \sim 80MW/m^2$ ).

The experiments are carried out by allowing for a dedicated leading edge facing the full parallel heat flux  $q_{||}$ . This setup is comparable to the case of a misalignment tolerance issue faced for the ITER Divertor [12]. Four samples mounted in the Ma-

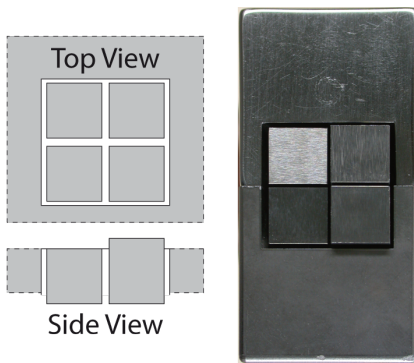


Figure 5: Sample configuration exposed in the AUG divertor manipulator. The sample edge length is 8 mm

nipulator are exposed to the Divertor, while the leading two are flush mounted the subsequent column has an additional 1.5 mm of material exposing a leading edge of each  $\sim (1.5 \times 8) mm^2$ . As seen in figure 5 the sample is exposed with the plasma streaming onto the leading edge from the lefthand side.

The leading edge has been chosen with a height of 1.5 mm as to facilitate melting while a typical leading edge at ITER by design would not be larger than 0.3 mm - facing however

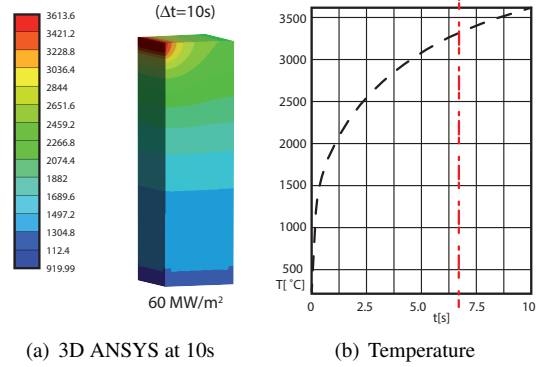


Figure 6: Simulated Temperature evolution for the in AUG exposed castellation with increased leading edge surface (1.5mm)

$q_{||} \sim 200MW/m^2$ . To significantly melt the exposed sample ANSYS calculations (Fig. 6) demonstrated that at  $80MW/m^2$  the exposed edge should suffice to melt well within the typical pulses duration of 6 s (fig. 3) while  $q_{||} \sim 60MW/m^2$  would fall short.

### 3. Results and Discussion

In the following section the main results with respect to material changes as well as plasma impact during the AUG exposures are discussed.

#### 3.1. Melt-Damage and Material Redistribution

With respect to material redistribution, material structure and damage the exposures in AUG as well as C-Mod show remarkable similarities (fig. 7). In both machines the melt layer mo-

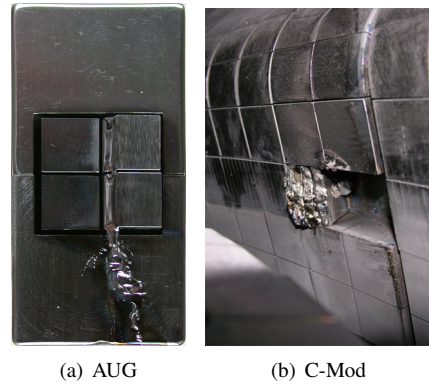


Figure 7: Post mortem pictures of the observed meltdamage after exposures in AUG and C-Mod

tion is downward following gravity and  $j \times B$  forces driven by thermoelectric emission [1]. In both cases no clear indication is given for plasma pressure driven melt layer motion on a large scale (cf. Sec. 3.3). The main difference here is the amount of molten material due to the different exposure conditions. While the amount of redistributed and lost material in the case of AUG is rather small (225 mg & 315 mg) - only 1 major melt event has occurred during the series of 3 pulses (#27377 - #27379) - the

amount of material lost in the case of C-Mod is roughly 15 g estimated from the volumetric loss measured ( 4 – 5 g from the lost tile, 11g from remaining tile). A large series of plasma discharges was run on or close to the exposed W-lamella causing significant redistribution and material loss. Figure 8 shows a

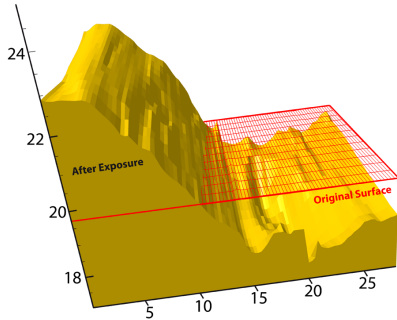


Figure 8: Three dimensional representation of the surface structures after melt resolidification and extraction of the 8th W-lamella damaged during the run campaign (cf. fig. 7(b))

comparison between the surface of an undamaged W-lamellae out of the W-row exposed in C-Mod and the 'lamella #8' as the most damaged one - as its front surface extended the farthest out from the nominal divertor surface (fig. 7(b)). Comparing the damage inflicted between the two divertor experiments, one main difference is clear: The AUG castellation melt is redistributed to the lower vertical surface of the manipulator away from the leading edge, basically depositing new hill structures on a previously pristine surface. In contrast the C-Mod redistribution is located on the lamellae itself, not bridging the gap to the next lower molybdenum tile, moving material downwards along the lamella building up to a height of several mm. When material moves out of the power bearing area, melt layer hills may be tolerated unless additional structures are exposed by material removal ( cascade failure - cf.15).

In both cases hill structures or edges are produced which being more prone to higher heat fluxes and thus potentially cause an deteriorating impact on further plasma operation by causing even more W to melt or be released from the surfaces. It can be seen that despite the different magnitudes of heat loads and melts both cases severely hamper further operation. (see below, [9]). It is not necessary to have large scale melt damage to cause disruptions due to melt layer loss as few  $\mu\text{g}$  of material can cause several 100 MW of radiated power [13, 2]. Apart from the obvious impact by material redistribution and material loss changes to the material structure such as grain growth, layer formation, bubbles or voids can have a severe impact on the material properties [1, 2].

### 3.2. Resolidification & Material Structure Changes

In both the AUG sample (fig. 9) and the C-Mod lamellae (fig. 10) there are clear indication of reduced power handling capability given that strong cracking as well as grain growth are observed. In figure 9 the cut was performed perpendicular to the jxB melt flow direction to characterize the changes to the leading edge, e.g. angle with respect to the unmolten shape,

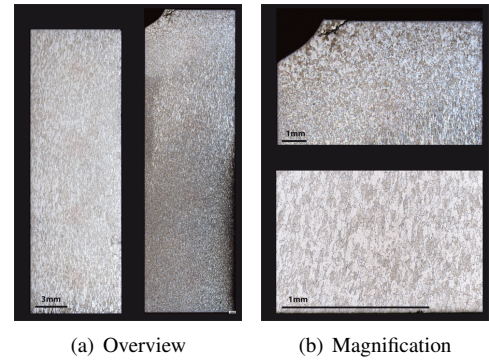


Figure 9: Metallurgical cut of the samples exposed during ASDEX pulses #27377 – 27379, (a) shows an overview of the two samples, while (b) is displaying a close up of the top and bottom parts of the molten castellation.

as well as the material changes, while for C-Mod the cut was performed along the lamella, thus along the flow of the melt.

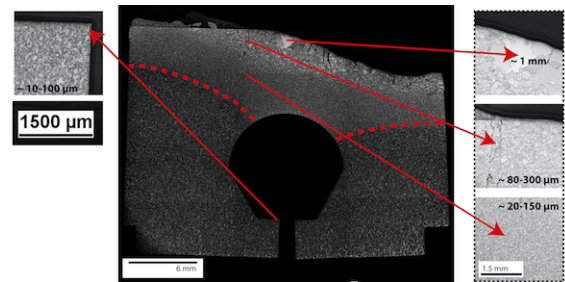


Figure 10: Metallurgical cut of one exposed W-lamella (#7) after the accidental melt incidents during the 2009 run campaign of Alcator C-Mod).

In both cases grain growth - re-crystallization up to the millimeter size, deep into the sample is observed, making the material much more brittle and prone to cracks. The material changes follow the temperature impact displayed in figures 9 & 10. The gradient in grain size follows the temperature gradient. Comparing with either the deep unexposed ends of the lamella or in case of AUG the flush mounted samples clearly shows the severe impact of melting on the grain size which changes by orders of magnitude. Despite the AUG sample only being exposed 3 times the depth of cracks is in the same order of magnitude as for the C-Mod sample. Multiple thermal cycling seems not to increase the effect on the material structure beyond the initial thermal impact (the initial cracks relieve the stresses of further melts like tiny castellations). The cracks reach a depth of several mm in the perpendicular direct with respect to the samples exposed top surface. Clearly the chance of losing parts of the material is increasing. In addition to the embrittlement and cracking in both AUG and C-Mod cases a loose layer of material exists on either the neighboring material surfaces or on the lamella. Such loose material, when impacted by additional heat flux in subsequent discharges is subject to 'explosive' (fig. 14, [9]) release due to minimal attachment to the surface. Having misalignments or unshaped surfaces will damage the material up to its destruction.

### 3.3. Melt Exposures and Plasma Impact

During melting especially the erosion of material (tungsten) and loss of larger pieces can impact plasma performance by launching large impurity 'projectiles' towards the core plasma. Plasma cooling by radiation and changing the concentration of impurities will influence the fusion burn in a future device [13]. Here, the impact of the plasma, through Edge Localized Modes (ELMs), on the melt layer stability and droplet release is discussed as well as the impact of a re-solidified melt and the subsequent exposure on the plasma stability / performance. Apart of the  $j \times B$  forces generally moving the melt along the target this material loss mechanisms due to ELMs can cause transport of material into the SOL and further into the main plasma causing reduction of fusion performance and radiation cooling. The typically allowed concentration of W in the core plasma is  $10^{-5}$  as given in [13].

In contrast to previous studies of melt layer loss behavior in AUG with a molten pin exposure [4, 7] a larger melt pool as seen from figure 9 is now subject to plasma impact. Studying the actual droplet dynamic after detaching from the melt is out of the scope of this paper and discussed in detail in [7]. Figure

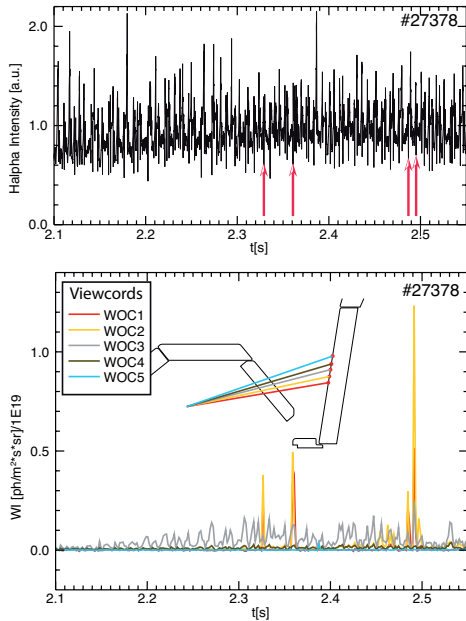


Figure 11: Spectroscopic measurements in the AUG Divertor during melt exposure (# 27378) - Top: Divertor  $D\alpha$  emission Bottom: Localized ELM induced tungsten source during initial melting.

11 shows the correlation of the local  $WI(400.9nm)$  line emission together with the  $D\alpha$  divertor recycling-signal during the ejection of droplets of tungsten. A spike on the  $D\alpha$  trace indicates an ELM occurrence which is an expulsion of plasma across the separatrix carrying particles and heat to the divertor. In the bottom part of figure 11, also showing the spatial distribution of the Spectroscopic observation channels, the time traces of the  $WI$  line intensity show clearly that localized in two channels distinct intensity spikes are visible, while the other channels are showing low signal or none. The trace of channel three is clearly correlated to the impact of plasma eroding

W in the divertor, each ELM spike shows a modulation of the  $WI$  signal typical for ELM induced tungsten erosion ([14]). For channels one and two only a few spikes are visible, still correlated with plasma impacting on the, in this case, molten surface. The above  $WI$  behavior indicates that some amount of the molten surface is ejected due to the impacting plasma pressure or  $j \times B$  forces connected to the ELM. This loss mechanism can cause transport of material into the SOL and further into the confined plasma causing reduction of fusion performance. Figure 12 demonstrates this by showing time-averaged local-

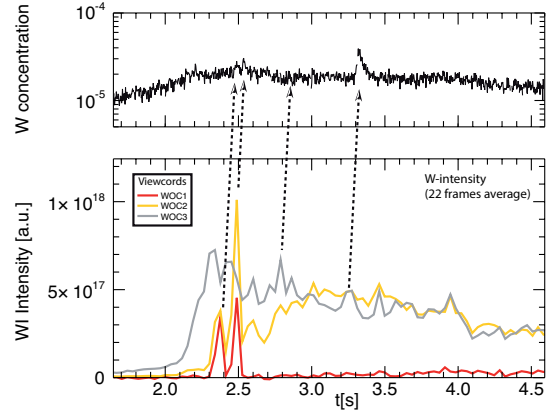


Figure 12: Spectroscopic measurements in the AUG main plasma and divertor during melt exposure (# 27378) - The Core W-concentration (Top) changes compared to local divertor tungsten emission ( $WI$  400.9nm) (Bottom) at the molten tungsten sample.

ized  $WI$  traces compared to tungsten concentration of the core plasma (top). With each spike on the local  $WI$  emission signaling a release of material to the divertor plasma a rise in tungsten concentration roughly 50-100ms later is observed. The local source can either be in the form of small droplets (2.3-2.5 s) or a steady stream of particles as seen in the later occurrence visible at 3.3 s. The effect of the melting and the connected ma-

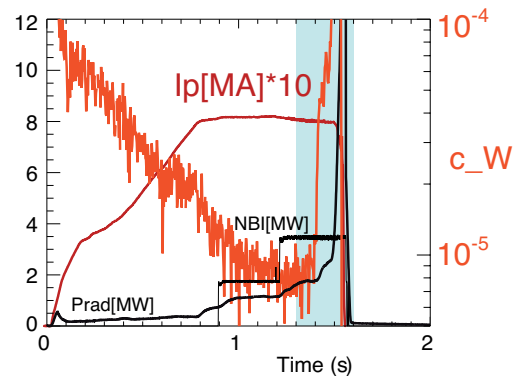


Figure 13: Evolution of plasma parameters incl. W core-concentration and radiated power causing a disruption after previous melt exposure in AUG.

terial re-distribution during #27378 on the subsequent plasma discharge (#27379) is displayed in figure 13. At 1.4 seconds a strong rise in the tungsten core concentration followed by an increase in radiated power is observed terminating the plasma.

Even though neither the full power nor the final position of the SP close to the Divertor manipulator was reached the material re-distributed to the lower parts of the manipulator (fig. 7) is already reached by large enough power to cause a loss of the re-solidified melt layer. From the fast camera clearly the material entering the divertor plasma can be observed, crossing all the way through the divertor also to the high field side target of the divertor. In an overlay of all droplet and particle traces observed

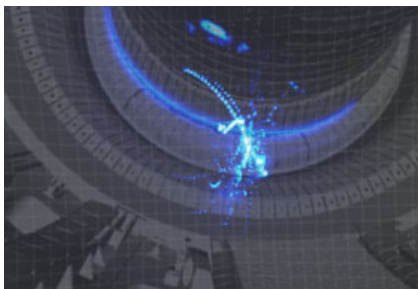


Figure 14: Convolution of images taken during the disruptive material loss in AUG ( #27379), following the initial melt exposure #27378

by the fast camera looking into the divertor figure 14 shows the explosive release of material. Similar to the issues faced in C-Mod (see above, [9] ) even a small melt damage on power bearing components can potentially release enough material causing the plasma to either disrupt or be at least severely hampered. In both AUG and C-Mod the disruptivity increases, in the case of C-Mod up to 100% while for AUG it rises only towards 30% - still intolerable for ITER. A tungsten source caused by melting thus needs to be avoided as it in the form of droplets [1, 2, 4, 7, 15] during the melt process or loss of re-solidified components.

#### 4. Conclusion and Outlook

From the above presented experiments several conclusions with respect to the performance of PFCs under melt conditions can be drawn in addition to the already presented results [1, 2, 4, 7, 15]. With leading edges exposed to the divertor plasma melting is almost unavoidable, thus shaping of divertor components intersecting with high heat and particle flux to remove leading edges is mandatory. In addition one needs to consider the impact of transient events on the melt process. While so far melting due to transient power flux, e.g. ELMs has only been simulated in plasma-gun experiments, it is clear that the impact of ELMs as observed in AUG shows the detrimental effect of material loss facilitated by transients in addition to the material change itself. With the melt redistributing along the direction of the  $j \times B$  moving perpendicular to the B-Field on the surface, hill structures arise containing highly in-homogenous material, prone to cracking, material loss and seriously degraded in power handling ability. In addition there is an increased probability of formation of additional impact edges. So far no experiment has been able to show plasma shaping of metallic PFCs in the sense of ameliorating the leading edges due to misalignment or accidental shifts in first wall components. In future experiments at AUG the potential amelioration or the possibility of a cascade failure of installed components shall be tested

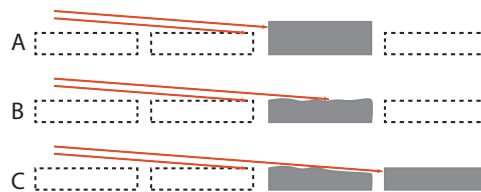


Figure 15: Schematic picture of potential situations arising from misaligned castellation(A) and subsequent melt damage amelioration (B) or cascade failure (C)

as displayed in figure 15. This experiment should answer the question whether a pre-existing leading edge (A) actually will be smoothed (B) or the subsequent castellation will be hit by the plasma flux due to the removal (C) of liquid material leading to an exposed surface? Initial findings can't exclude either scenario while so far showing no indication for smoothing. In summary melting needs to be avoided as droplets can, and will, enter the core plasma; even small amounts can hamper the fusion performance. Avoiding molten surfaces seems possible by shaping the PFCs before installation, while no in-situ smoothing has been observed so far. Of course, even in the case of a properly designed PFC with shaping, imperfections in the material properties can possibly lead to a leading edge with subsequent problems due to melting. Cascade failure of components even though not yet observed needs to be avoided as this would cause a costly large scale repair of components.

#### Acknowledgement

This work, supported by the European Communities under the contract of Association between EURATOM/FZJ, was carried out within the framework of the EFDA Task Force on Plasma-Wall Interactions. The views and opinions expressed herein do not necessarily reflect those of the European Commission. This work is part of the joint experiment DSOL-25 under the International Tokamak Physics Activity. Special thanks to the team of the IEK-2 for their effort in supporting experiments and post-mortem analysis.

- [1] Coenen, J. W. et al. *Nuclear Fusion*, **51** (2011), 8, 083008.
- [2] Coenen, J. W. et al. *Nuclear Fusion*, **51** (2011), 11, 113020.
- [3] Tokar, M. et al. *Nuclear Fusion*, **52** (2012), 013013.
- [4] Krieger, K. et al. *Journal of Nuclear Materials*, **451** (2011), 211.
- [5] Bazylev et al., B. *Physica Scripta*, **T145** (2011), 014054.
- [6] Coenen, J. W. et al. *Fusion Science And Technology*, **61** (2012), 2, 129–135.
- [7] Krieger, K. et al. *Physica Scripta*, **T145** (2011), 014067.
- [8] Barnard, H.; Lipschultz, B. and Whyte, D. *Journal of Nuclear Materials*, **415** (2011), 1, Supplement, S301 – S304.
- [9] Lipschultz, B. et al. *This conference - PSI 2012*, (2012).
- [10] Weinlich, M. e. a. *Europhysics Conference abstracts Proc. , 23rd EPS Conf. on Controlled Fusion and Plasma Physics*, **20G/part2** (1996), 715–8.
- [11] Geier, A. et al. *Plasma Physics and Controlled Fusion*, **44** (2002), 10, 2091.
- [12] Pitts, R. A. et al. *Journal of Nuclear Materials*, **415** (2011), 957–964.
- [13] Puetterich, T. et al. *Nuclear Fusion*, **50** (2010), 2, 025012.
- [14] Dux, R. et al. *Nuclear Fusion*, **51** (2011), 5, 053002.
- [15] Coenen, J. W. et al. *Journal of Nuclear Materials*, **415** (2011), 78–82.